International Journal of Engineering & Technology, 7 (4.39) (2018) 608-614

International Journal of Engineering & Technology

Website: www.sciencepubco.com/index.php/IJET

Research paper

Study of Size, Shape and Nanoparticle Concentration Effect in Micro-Channel, Pillar and Flat Channel

Ass. Prof. Debashis Dey[1]

Department of Mechanical Engineering, ITER,SOA(Deemed to be University), Bhubaneswar, India[1]
**Corresponding author E-mail: debashisdey@soa.ac.in:*

Abstract

In this study,thermal efficiency was calculatedbased on experimental results of micro channels, flat channel and pillars. Here constant heat flux was applied from the bottom of the test section using film heaters where DC (Direct Current) power was supplied to the heaters and a lamp was used for radiation experiments. The flow through channels and pillars were maintained at constant rate using two syringe pumps. There were eight thermocouples for heater and six thermocouple for radiation to measure the temperature continuously using DAQ (Data Acquisition) system at different locations of the test section. Pressure drop between inlet and exit was recorded using calibrated pressure sensor and the reading was fed to the DAQ system. There were different fluids like DI (De-Ionized) water, 0.05%TiO_2 (Titanium di-Oxide), 0.1%TiO_2 and again water was used for testing. Similar series of tests were carried out with SiO_2 (Silica) as well. It has been found that nano-fluid has significant effect (it is termed as the "nanofin effect") on effective convective heat transfer as it creates "Nanofin" on the substrate surface and effectively increase the area for heat transfer. However, after a certain concentration of nano-fluids, the effective area for fluid passage also decreases and thus convective heat transfer decreases. This is why water repeat case gives best result among all four cases on heat transfer.

***Keywords**: Nanofluid, Micro-channel, Convective Heat Transfer, Radiative Heat Transfer.*

1. Introduction

Solar energy is one of the promising alternative energy options in near future. As conventional energy sources e.g. coal, oil and gas are going to be depleted soon; this area needs to strengthen to harvest the energy from the Sun. Solar energy can be of two types e.g. Solar Photovoltaic and Solar Thermal energy. Solar thermal takes the energy from the Sun for a wide spectrum of wavelengths of energy than Solar Photovoltaic. That is why efficiency of this type of system can reach much higher value (can be greater than 50%) than Solar Photovoltaic (~ 15-20%). Solar thermal energy can be used for building applications as well. This can make the building self-sustainable. Windows with micro-channel, pillar or flat channel inside that can be used for the building. Here nanofluid through this micro channel can be used for solar energy harvesting. Nanofluid can enhance the energy gain from the Sun. Because from different literatures, it is found that a small fraction of nanoparticle doping in the base fluid can enhance the thermo-physical properties. This way, the energy requirement for heating the water can be reduced as well as cooling load for the building will also be less. As there will be very small amount of nanoparticle concentration, so building window visibility will not be affected whereas at the same time high heat flux can also be removed using nanofluid.

Research in efficient thermal management of high heat flux devices are becoming popular with the advancement in micro/nano technologies (MNT). There are many such kind of devices e.g., lap-on-chip, high power lasers, laser diodes, batteries, fuel cells, laser cutter etc. The main objective of the miniaturization of these devices is to make the system compact and portable. These compact devices have higher volume to surface ratio than conventional devices i.e. for the same volumetric heat generation available cooling surface area is reduced. This will increase the operational temperature of the device and sometimes hot spot can form due to uneven temperature distribution and inefficient cooling of the devices. Thus, performance of the device may deteriorate or failure may take place. If the temperatureis high, fluctuation and large number of hot spots, then laser diodes and computer chips may stop functioning properly (Mahajan R. et al. [1]). There are incidents of damage and explosion for lithium batteries if operating temperature is not maintained properly (Baker J. [2], Hadjipaschalis I. et al. [3]). Therefore, proper thermal management of these devices is important for the design of system size and efficiency.

There are different heat dissipation techniques e.g., forced convection of air over heat sinks, natural convection of air over heat sinks, immersion in non-conducting oil, forced convective heat transfer using liquids (single phase or multi-phase type).There are limitations for each techniques. Air is a poor conductor of heat and this is only low level of heat dissipation. Similarly, non-conducting oil makes the whole set up clumsy. Heat sinks take a lot of space. Even though forced convection has its limitation, it is cheap, reliable and effective technique and so, lot of studies are carried out for cooling using forced convection.

Convective heat transfer can be enhanced by the following techniques:

a) Increase the effective surface area
b) Increase the thermal properties of flow media
c) Proper convection techniques

Among all the techniques mentioned above, forced convection using liquids through micro channels is the most effective technique. In general, solid materials have higher thermal

conductivity than liquid materials. Therefore, liquid-solid mixture or colloidal suspension of nano particle in nano fluid enhances thermal properties of the fluid. These nano particles form nanofin and increase the effective surface area as well.

Eastman J. A. et al. [4] found that 40% enhancement in thermal conductivity with only 0.3% volume of Cu nanoparticles doping in ethylene glycol. Shin D. et al. [5] found more than 100% enhancement in specific heat capacity for nanofluids due to compressed phase, needle like structure and percolation network. If this behavior of nanofluid can be used for, window-application then that will not only save the energy requirement for the building but also reduce the pollution indirectly. As small portion of nanoparticle will be used, so the cost involvement will not be much and same fluid can be used in a loop. Thus, the free solar energy can develop sustainable buildings for future.

Eastman suggested colloidal suspension of nanoparticles in a conventional heat transfer fluid as stable fluid for the enhancement in thermal properties (Choi S. U. S. et al. [6]).This stable colloidal liquid, which has suspended nanoparticles, is known as "nanofluids". After that it has become a popular research topic in the past two decades for various applications e.g., coolants, thermal energy storage materials, lubricants, emulsifiers or biomedical drug delivery agents. Nanofluids are an innovative heat transfer fluid and have been intently studied over the past two decades. Their heat transfer augmentation is mainly due to a small concentration of nanoparticles that dramatically change or enhance the thermo physical properties of the base fluid. These nanofluids are comprised of a base liquid such as water, ethylene glycol, propylene glycol, or oil and a small volume fraction of some metal, metal oxide, or ceramic, as well as other materials, with particle size ranging from 1 to 100 nm. Popular particles include chemically stable metals (i.e. Ag, Au, and Cu), metal oxides (TiO_2, SiO_2, CuO, Al_2O_3, ZrO_2), or carbon (diamond, graphite, CNT, fullerene), etc. Most suspensions contain less than 4% by weight or volume of the nanoparticle (Singh et al. [7]).

2. Literature Review

VafaeiS. et al. [8] studied the effect of particle concentration, initial sub cooling and mass flux on CHF (Critical Heat Flux) of a single Stainless Steel micro-channel (510 µm internal diameter and 306 mm length). Here Al_2O_3 particles (average diameter was 25nm) were suspended in deionized water with varying volume fraction 0.001 -0.1%. Two probable factors are considered here e.g. modification of the heating surface through particle deposition and modification of bubble dynamics through particle suspension in the liquid. Different sub cooling are maintained by preheating the working fluid and mass flow rate range was 600-1950 kg/m^2-s. The experimental set up is shown in Figure (1) below:

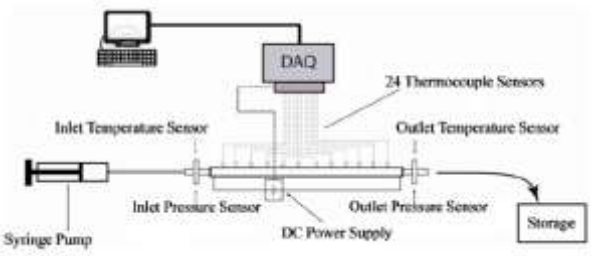

Figure 11: Schematic of experimental set-up, VafaeiS. et al. [8]

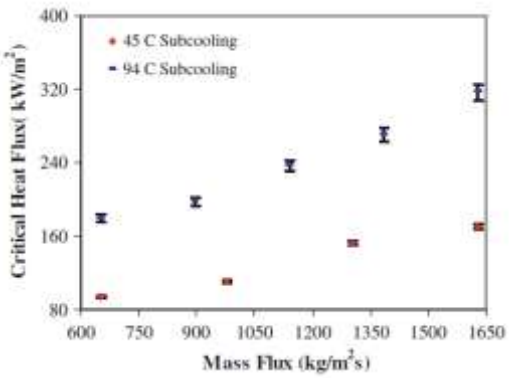

Figure 2: Variation of CHF of DI water with mass flux and sub-cooling, Vafaei S. et al. [8]

There was increase in CHF with mass flow rate and sub-cooling as shown in above Figure (2).

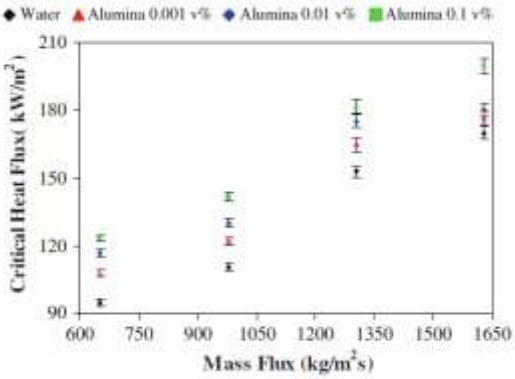

Figure 32: Variation of CHF with mass flux and nanoparticle concentration at 45°C sub-cooling,VafaeiS. et al. [8]

With the increase in nanoparticle concentration and mass flux, CHF enhances as shown in Figure (3).

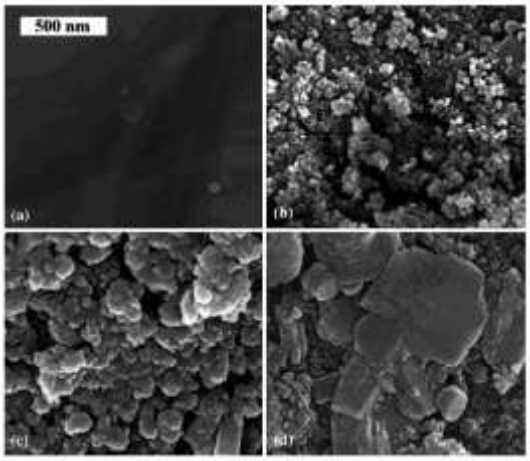

Figure 4: SEM (Scanning Electron Microscopy) pictures of the test section of stainless steel micro-channel close to the outlet after experiments with a) boiling water b) 0.001 vol% c) 0.01 vol% d) 0.1 vol% Al_2O_3, VafaeiS. et al. [8]

SEM images in Figure (4) showed significant nanoparticle deposition in the micro-channel exit. The reasons behind the increase in heat transfer can be particle deposition, surface morphology modification (modification of force balance at the triple line), and a change in the wettability and bubble contact angle.

Xu L. et al. [9] carried out the experiment to check the bubble effect on pressure drop and to understand the bubble dynamics when nanofluid was passed through micro-channel. Here 0.2% by

weight γ-Al_2O_3 (Φ~40nm)-DI water was used as a nanofluid. Nanofluid preparation and SEM, TEM images were taken to show the particle size. The particle size distribution was not checked. The simple mixing rule was used for the specific heat capacity calculation and Einstein's model was used for viscosity measurement. However, the nanofluid behaved as non-Newtonian fluid.

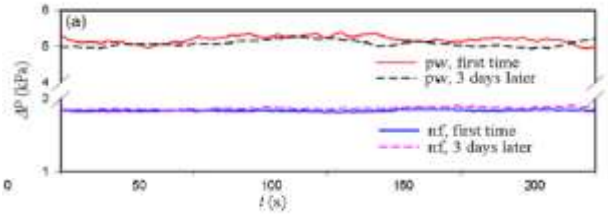

Figure 5: Pressure drop (for both pure water and nanofluid) in the micro-channel vs. time at mass flux 171 kg/m^2-s and heat flux 400 W/cm^2 (T_{in} = 27°, T_{out}=52.6°C (pure water) and T_{out}=53.4°C (nanofluid)) , Xu L. et al. [9].

Figure (5) showed that there was more pressure drop when water was used instead of nanofluid through micro-channel, which is not conventional.

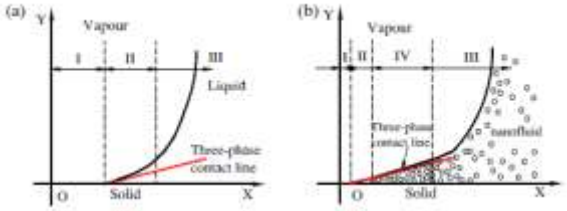

Figure 6: Solid-liquid-vapor three-phase contact line for a) Pure Water b) Nanofluid, Xu L. et al. [9]

In Figure (6), Region I is the area between the heater surface and the dry vapor, region II is thin liquid film region without nanoparticles, region III is the bulk nanofluid region and region IV is the thin liquid film evaporation heat transfer region with nanoparticles involved. Nanofluids decrease region I and II but increase region III; thus, heat transfer performance improves.

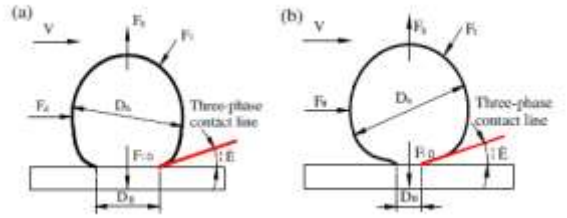

Figure 7: Force balance acting on the growing bubbles a) Pure Water run b) Nanofluid run, Xu L. et al. [9]

As shown in Figure (7), force balance equation for the bubble is as per Equation (1):

$$F_\sigma + F_i \text{ (both liquid and vapor inertia force)} = F_g \text{ (buoyancy force)} + F_d \text{ (viscous drag force)} \quad (1)$$

Surface tension force is given by Equation (2):

$$F\sigma = \sigma D_B \pi \mathrm{Sin}\theta \quad (2)$$

Where, D_B is the bubble departure diameter.
The surface tension for pure water and nanofluid remains same but D_B decreases for nanofluid case because of structural disjoining pressure and thus surface tension force decreases. Pressure difference between vapor and outside was evaluated using the following Equation (3):

$$p_l - p_v = -\frac{\sigma\left(\frac{d^2H}{dx^2}\right)}{\left[1+\left(\frac{dH}{dx}\right)^2\right]^{\frac{3}{2}}} - \Pi(H) + \Delta\rho g H + \frac{q^2}{2\rho_v h_{lv}^2} \quad (3)$$

Π(H) is the structural disjoining pressure, which pushes the solid-liquid-vapor contact line to the vapor side and these phenomena, decreases the contact area between the heating surface and dry vapor. This pressure happens due to molecular forces between nanoparticles and water that are not present for pure water case.

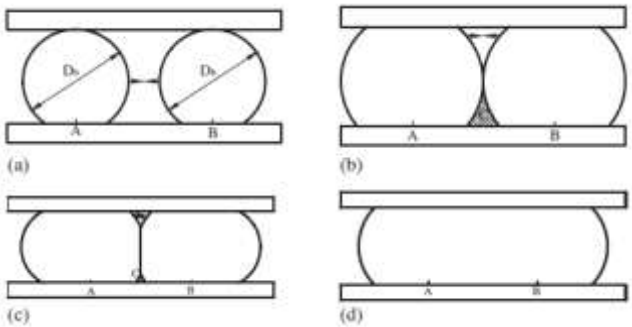

Figure 8: Merging of two neighboring bubbles, Xu L. et al. [9]

As we saw that bubble size for pure water was bigger before departure but the micro-channel size was confined, thus bubbles were elongated. When these two elongated bubble tip contacts coalescence starts and further growth decreases the presence of liquid at corners and a big merged bubble forms (Figure (8)). This bubble will break up and miniature bubbles will form after some time. In a micro channel bubble coalescence happens for both pure water and nanofluid cases but this coalescence frequency is more for pure water i.e. nanofluid stabilizes the boiling flow. When elongated merge bubble appears pressure drop increases and miniature bubble reduces the pressure drop. As this change in bubble size frequency is less for nanofluid, thus pressure drop will also be less. Nanofluid also reduces the dry patch formation between the heater surface and vapor phase and thus the heat transfer enhancement happens. So, nanofluid can be used for forced convection in a micro-channel with low concentration.

3. Experimental Set-Up

Experimental set up has the following parts:

a) Micro Channel/Pillar/Flat as substrate (Figure. (10))
b) Syringe Pump (Pump 11 Pico Plus, Havard Apparatus)
c) Film Heater (KHR-2/10-P, Omega)
d) DC Power Supply (SPS 200-50-K025, American Reliance Inc.) (Fig.1)
e) DAQ (Data Acquisition) System (NI SCXI-1303, National Instrument)
f) Thermocouples (4 nos. each at inlet and exit)
g) Inlet and Outlet Port assembly
h) Pressure Sensor and its power source
i) IR (Infra-Red) Camera
j) TiO_2 as nano particle (0.05% and 0.1% by weight)
k) DI (De-Ionized) water
l) JB weld
m) Styrofoam
n) Fiberglass

Details of different components are shown below in Figure (9) and Figure(10) respectively.

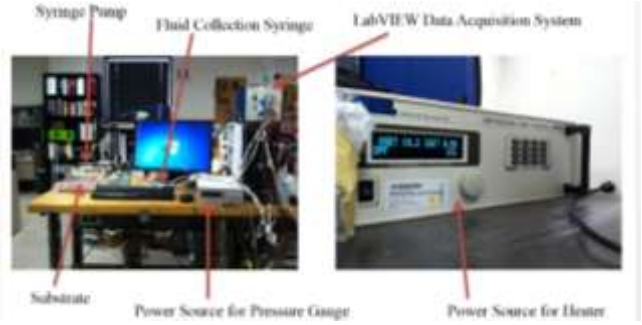

Figure 9: Testing apparatus for the experiment

Four different heater settings were used for the experiment i.e. 10W, 30W, 40W and 50 W respectively using DC power supply.

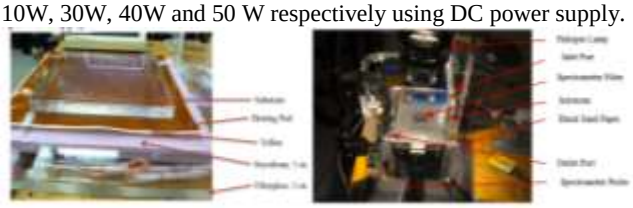

(a) (b)

Figure 10: (a) Micro-channel with heating pad at the bottom and (b) Radiation set up with Spectrometer probe

Syringe pump was used to maintain three different constant flow rates i.e. 10ml/hr, 15ml/hr and 20ml/hr respectively through the substrates. Different sizes of micro channel, pillar and flat are used as shown in Table (1).

Table 1: Dimensions of the Substrates

Type	Etch Depth (μm)	Width (μm)	Pitch (μm)	Symbol
Micro Channel	15	50	100	C5, C9
	35	100	200	C1, C13
	75	200	400	C4, C11
Pillar	50	-	2000	P14
	150	-	2000	P7
	200	-	2000	P6
Flat	150	-	2000	F15, F16

Pressure drop between inlet and outlet port is measured using pressure sensor (different sensors were used based on the pressure drop) and temperatures are recorded using automated high acquisition apparatus with a sampling rate of 200 Hz using LABVIEW® control software.

During the experiment unsteady and steady, both data are recorded. Unsteady state recorded one data per second until it became steady state. In this experiment steady state refers to if the data does not change more than one unit over five minute span then system attains steady state.Once a steady state is achieved, the acquisition system is changed to record 200 data points per second and an infrared image is taken of the substrate. Infrared camera is set to 0.93 emissivity to view the temperature distribution of the substrate keeping focus at the center of the substrate.

4. Results and Discussion

For each set of experiment, following graphs for three flow rates are generated:

a) Temperature Inlet (T_{in}, °C)
b) Temperature Outlet (T_{out}, °C)
c) Change in Temperature (ΔT_{io},°C)
d) Heat Flux (q", W/m^2)
e) Energy Out (E_{out}, W)
f) Efficiency (%)
g) Pressure Drop (ΔP, Pa)

Experiments are carried out for both the radiation and the heaters cases. The main objective is to compare radiation data with the heater case (base case) and how suitable radiation data is for solar application. Details of the experimental results are discussed below. In case of heater and radiation experiments, total 277 and 291 experiments were carried out respectively.

4.1 Heater Experimental Results

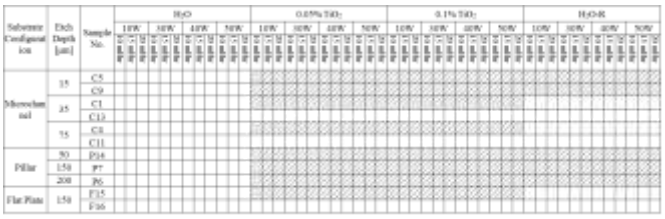

Figure 11: Heater Experiment Matrix

Here different power supply, flow rates, micro channel, pillar and flat plate cases (shape effect) are considered for the heater experiments as shown in the above Figure (11).

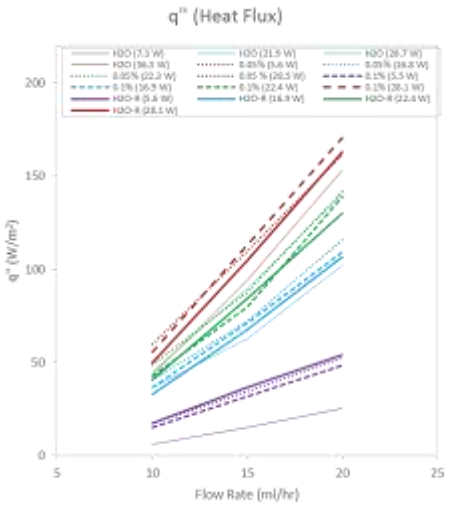

Figure 12: Heat flux gain by fluids for micro-channel C11

Heating pad is bigger in size than the substrate and thus heat flux is adjusted accordingly. Heat flux is calculated based on the following equation:

$$q" \text{ (W/m}^2) = \frac{q"_s A_s}{A_p} \quad (4)$$

Where $A_s$is the bottom area of the substrate and A_p is the area of the heating pad. With the increase in flow rate and heat supply, heat flux gain increases (Figure (12)). This heat gain is much higher for micro channel cases than flat plate case.

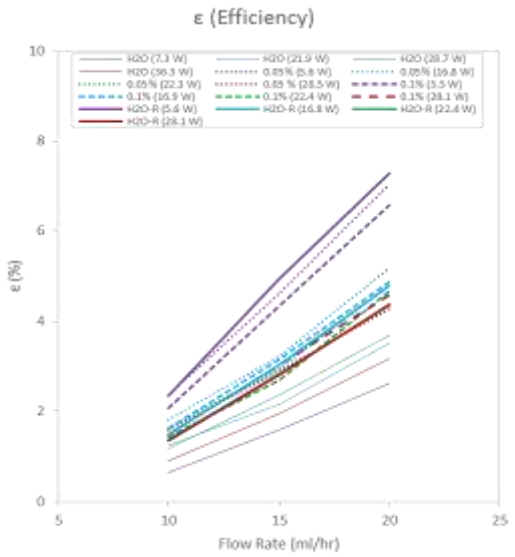

Figure 13: Efficiency for C11 micro-channel

Efficiency is calculated based on following equation:

$$\text{Efficiency, } \eta\ (\%) = \frac{100E_{out}}{q"A_s} \quad (5)$$

Efficiency is the best when flow rate is maximum (20 ml/hr) but heat flux is minimum e.g., H_2O-R for 5.6W has the highest efficiency (~8%) as shown in Figure (13). Water repeat case gives much better efficiency than 0.1%TiO_2 case. There may be the optimum nanoparticle concentration beyond that heat convection decreases instead of enhancement.

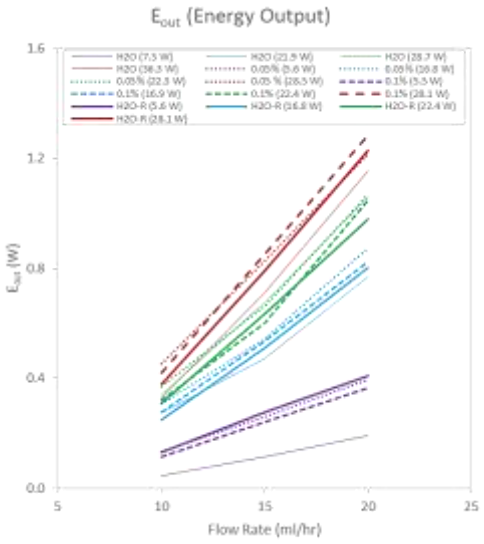

Figure 14: Energy Out for C11 micro-channel

Heat gain by fluid is given by following equation,

$$E_{out} = mC_p\Delta T_{io} \quad (6)$$

As it is found before that temperature gain is proportional to flow rate and heater power supply, so energy gain is maximum for highest flow rate and the maximum heater power supply case as shown in Figure(14).

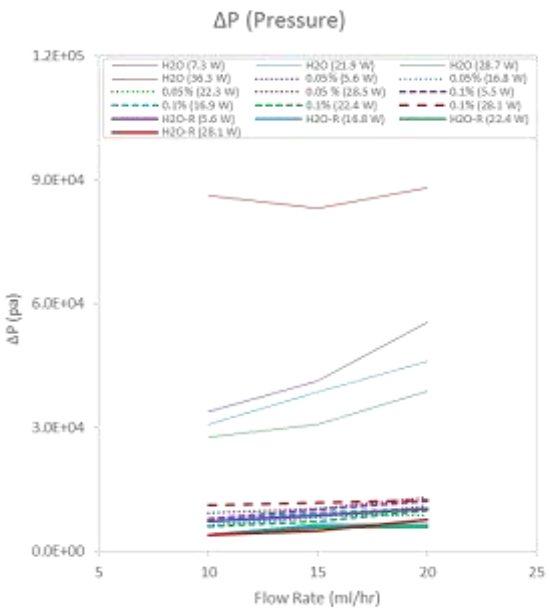

Figure 15: Pressure Drop for C11 micro-channel

Among all the four cases, pressure drop is minimum for flat case as it has higher etch depth and pitch in comparison to channel cases as shown in Figure(15). This pressure drop remains almost constant for high etch depth channel and low heat flux case. As the etch depth decreases for micro channel case pressure drop increases a lot. This is also interesting to note that for the flat case if nanofluid is passed through then pressure drop will be almost one third than only water. Nanoparticle helps to reduce the bubble size and thus less pressure drop takes place.

4.3 Radiation Experimental Results

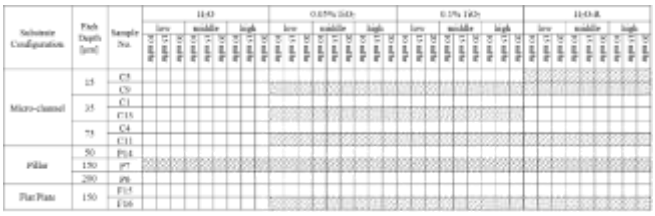

Figure 16: Radiation Experiment Matrix

Similar to heater experiments, different power supply, fluid flow cases, micro channel, pillar and flat plate cases are considered for the radiation experiments as shown in the above Figure (16).

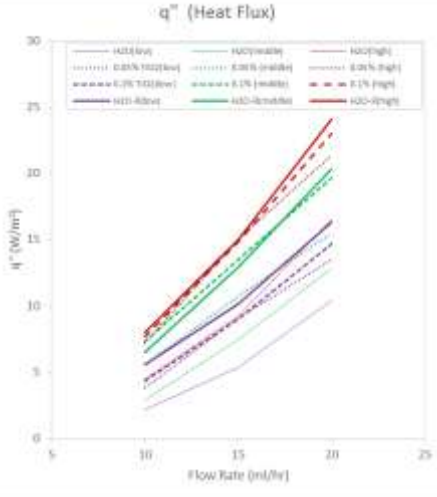

Figure 17: Heat Flux Gain for C4 micro-channel

Heat flux gain is proportional to the flow rate and radiation intensity. Again, water repeat case has higher heat flux gain than all the other cases and it is maximum for high radiation intensity as shown in Figure(17).

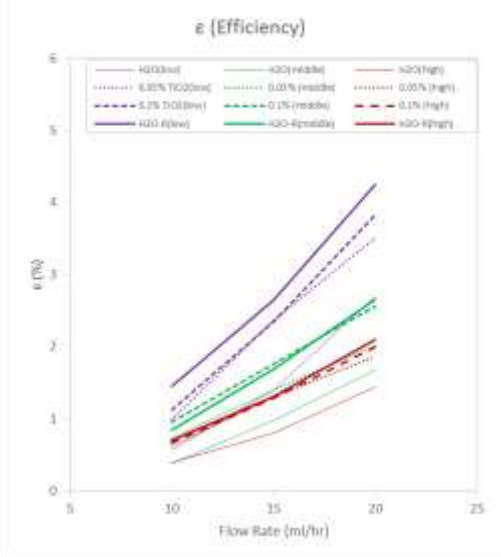

Figure 18: Efficiency for C4 micro-channel

Here efficiency for different radiation intensity cases are calculated based on the assumption that the effective high radiation is 10% of lamp maximum power. The maximum power for the lamp is 250W. For low and medium radiations, effective radiations are one third and two third of high radiation respectively. Energy gain is calculated based on equation (3) and the ratio of these parameters (energy gain and effective radiation intensity). Here efficiency is proportional to the flow rate but inversely proportional to the radiation intensity as shown in Figure (18).

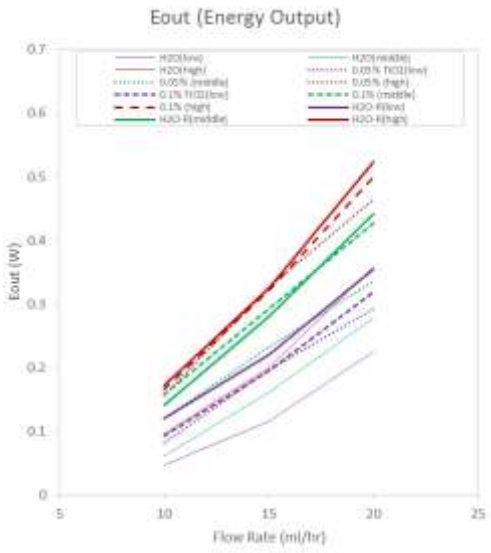

Figure 19: Energy out for C4 micro-channel

Energy out is calculated based on the equation (3). This energy is proportional to the flow rate, radiation intensity etc. and the energy gain by the fluid maximum for water repeat case as shown in Figure (19).

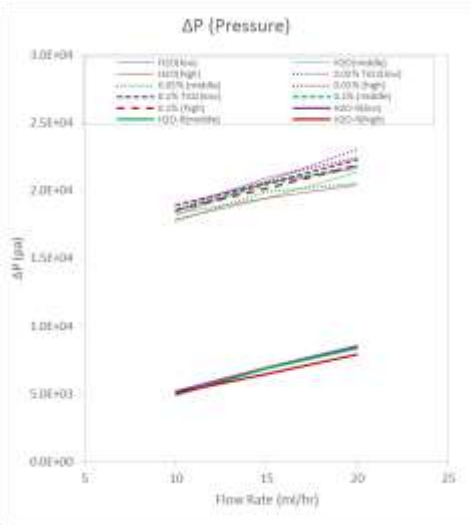

Figure 20: Pressure drop for C4 micro-channel

Pressure drop is constant for C4, P6 and P14 cases, but it increases with high flow rate for C1 micro-channel as shown in Figure(20). This drop is random for flat case. There is no pattern for flat case for pressure drop because of bubble's growth and collapse creates lot of pressure fluctuations.

From different nanofluid case studies, it is found that water has the highest efficiency for both micro-channel and pillar cases, but in case flat plate case 0.05% TiO_2 gives the maximum efficiency. In most of the cases, water repeat has higher efficiency than water case only.

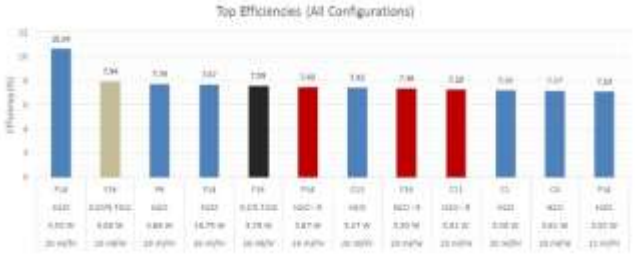

Figure 21: Efficiency variation for heater cases considering all configurations

The highest efficiency was obtained with H_2O in the pillar configuration at the highest flow rate and lowest heat input as shown in Figure(21). In case of only micro-channel, the highest efficiency is found for C13 micro-channel with water only. In case of only pillar, Pillar case (P14) gives the maximum efficiency for the lowest radiation and the highest flow rate. In case of flat plate, the highest efficiency is found for with 0.05% TiO_2 nanofluid case, maximum flow rate and lowest radiation.

Despite more tests being run in the micro-channel (C) configuration, the best efficiencies were typically seen in the pillar (P) configuration. Flat case is also comparable with channel case but there is blow up of bubbles when heat flux is high and thus steady state is difficult to attain at that condition.

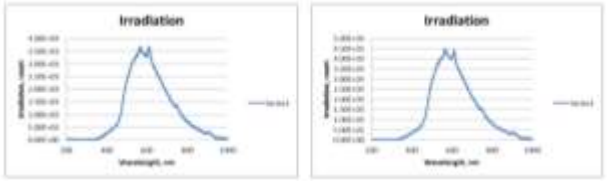

Figure 22: Comparison between irradiation with substrate and irradiation without substrate

Irradiation is measured using the fiber optics spectrometer; the graph is plotted for both with substrate and without substrate cases (Figure (22)). This is single probe measured plot. It is found that

both have same nature of profile but with substrate case has less number of irradiation count than without substrate case. Area integration under the curve gives heat flux value i.e. less heat flux is passed through and reaches the probe when substrate is present. It is because the difference in irradiation count is absorbed by the substrate. This is noteworthy that this data is not calibrated one. Therefore, it gives only qualitative change in heat flux.

4.4 Measurement Uncertainty

Energy out is calculated based on the following equation

$$E_{out} = \rho \, V \, C_p(T_2 - T_1) \quad (7)$$

The measurement uncertainty for energy out is given by the following equation (Kline and McClintock (1953))

$$\frac{\omega_{E_{out}}}{E_{out}} = \left(\left(\frac{\omega_v}{v}\right)^2 + \left(\frac{\omega_{T_2}}{T_2 - T_1}\right)^2 + \left(\frac{\omega_{T_1}}{T_2 - T_1}\right)^2 + \left(\frac{\omega_\rho}{\rho}\right)^2 + \left(\frac{\omega_{C_p}}{C_p}\right)^2\right)^{\frac{1}{2}} \quad (8)$$

Heat supply is given by $q'' = (q_s'' x A_s)/A_p$, where $q_s'' = f(V,I)$ (9)

The measurement uncertainty for the heat supply (for the heater case) is given by

$$\frac{\omega_{q''}}{q''} = \left(\left(\frac{\omega_V}{V}\right)^2 + \left(\frac{\omega_I}{I}\right)^2\right)^{\frac{1}{2}} \quad (10)$$

Efficiency is given by, $\eta = 100 * E_{out} / q''$ (11)

The measurement uncertainty for efficiency is given by

$$\frac{\omega_\eta}{\eta} = \left(\left(\frac{\omega_{q''}}{q''}\right)^2 + \left(\frac{\omega_{E_{out}}}{E_{out}}\right)^2\right)^{\frac{1}{2}} \quad (12)$$

Where error in measured parameters are as follows:
ω_v : Range in measurement error in flow rate is ±0.1 ml/hr.
ω_V: Range in measurement error in voltage is ±0.1V
ω_{T1} : Range in measurement error in inlet temperature for bead thermocouple is ±0.05°C
ω_{T2} : Range in measurement error in outlet temperature for bead thermocouple is ±0.05°C
ω_ρ : Range in measurement error in density is ±1%
ω_{Cp} : Range in measurement error in specific heat is ±1%
ω_I : Range in measurement error in current is ±0.01A
So, error in energy out will be ±1.87% for minimum flow rate and minimum heat supply and ±2.18% error for minimum heat supply. So, for the efficiency total error will be ±2.87%. Here only one sigma error is considered for the above mentioned calculation.

5. Summary and Conclusion

Best efficiency is found for pillar case at lowest heat flux and maximum mass flux because a) Pillar acts as vortex generator, b) At low heat flux precipitation is minimum, c) At high mass flux heat transfer rate is high. At low concentration, nanofin-formation enhances heat transfer and at high concentration, fouling due to too much deposition affects heat transfer.

Water repeat case has better efficiency over 0.1% TiO_2 case. However, there is improvement (for the same heat flux) in efficiency from H_2O to 0.05% TiO_2 for 75µm etch depth micro channel. Therefore, there may be an optimum nano particle concentration for a particular geometry of channel or pillar.

In general η (water repeat)> η (0.1%TiO_2)> η (0.05%TiO_2)> η (water). Nanofin effect dominates over the nanoparticle effect on nanofluid. Spectrometer result reveals that there is 22% reduction in peak irradiation count for radiation passing through substrate over the without substrate case.

References

[1] R.Mahajan, C. Chiu, G Chrysler, Cooling a micro-processor chip, Proceedings of the IEEE, Volume 94, Issue 8,August 2006, PP 1476 – 1496.

[2] J. Baker, New technology and possible advances in energy storage, Energy Policy, Volume 36, Issue12, December 2008, PP 4368 – 4373.

[3] I. Hadjipaschalis, A. Poullikkas, V. Efthimiou, Overview of current and future energy storage technologies for electric power applications, Renewable and Sustainable Energy Reviews, Volume 13, Issues 6-7, August-September 2009, PP 1513 – 1522.

[4] J. A. Eastman, S. U. S. Choi, S. Li, W. Yu, L. J. Thompson,Anomalously increased effective thermal conductivities of ethylene glycol-based nanofluids containing copper nanoparticles, Applied Physics Letters, Volume 78, Issue 6, February 2001, https://doi.org/10.1063/1.1341218.

[5] D. Shin, D. Banerjee, Enhancement of specific heat capacity of high temperature silica nanofluids synthesized in alkali chloride salt eutectics for solar thermal energy storage applications, International Journal of Heat and Mass Transfer, Volume 54, Issues 5-6, February 2011, PP 1064 – 1070.

[6] S. U. S.Choi, J. A. Eastman, Enhancing thermal conductivity of fluids with nanoparticles, ASME IMECE,November 12 – 17, 1995.

[7]]N. Singh and D. Banerjee, Nanofins: Science and Applications, New York: Springer, 2014.

[8] S. Vafaei and D. Wen, Flow boiling heat transfer of alumina nanofluids in single microchannels and the roles of nanoparticles, Journal of Nanoparticles Research, Volume 13,Issue 3, PP 1063-1073, March 2011.

[9] L. Xu and J. Xu, Nanofluid stabilizes and enhances convective boiling heat transfer in a single microchannel, International Journal of Heat and Mass Transfer, Volume 55, Issues 21-22, PP 5673-5686, October 2012.

[10] S.J. Kline, F.A. McClintock, Describing uncertainities in single sample experiments, Mechanical Engineering 1, ASME, 1953.